# Feasibility of estimation of brain volume and 2-deoxy-2-18F-fluoro-D-glucose metabolism using a novel automated image analysis method: Application in Alzheimer's disease

Erik S. Musiek[1*] MD, PhD,

Babak Saboury[2*] MD, MPH,

Shipra Mishra[2] BS,

Yufen Chen[3] PhD,

Janet S. Reddin[2] PhD,

Andrew B. Newberg[2] MD,

Jayaram K. Udupa[2] PhD,

John A. Detre[1, 2, 3] MD,

Frank Hofheinz[4] PhD,

Drew Torigian[2] MD, MA,

Abass Alavi[2] MD, MD(Hon), PhD(Hon), DSc(Hon)

*1. Department of Neurology,*
*2. Department of Radiology and*
*3. Center for Functional Neuroimaging, University of Pennsylvania, 3400 Spruce St., Philadelphia, PA 19104*
*4. PET Center, Helmholtz-Center Dresden-Rossendorf, Dresden, Germany*
*\*Co-first authors*

\*\*\*

**Correspondence address:**
Dr. Abass Alavi, Division of Nuclear Medicine, Department of Radiology, Hospital of the University of Pennsylvania, Philadelphia, PA 19104, USA.
Email: Abass.Alavi@uphs.upenn.edu

## Abstract

The development of clinically-applicable quantitative methods for the analysis of brain fluorine-18 fluoro desoxyglucose-positron emission tomography (18F-FDG-PET) images is a major area of research in many neurologic diseases, particularly Alzheimer's disease (AD). Region of interest visualization, evaluation, and image registration (ROVER) is a novel commercially-available software package which provides automated partial volume corrected measures of volume and glucose uptake from 18F-FDG PET data. *We performed a pilot study of ROVER analysis* of brain 18F-FDG PET images for the first time in a small cohort of patients with AD and controls. Brain 18F-FDG-PET and volumetric magnetic resonance imaging (MRI) were performed on 14 AD patients and 18 age-matched controls. Images were subjected to ROVER analysis, and voxel-based analysis using SPM5. Volumes by ROVER were 35% lower than MRI volumes in AD patients (as hypometabolic regions were excluded in ROVER-derived volume measurement ) while average ROVER- and MRI-derived cortical volumes were nearly identical in control population. Whole brain volumes when ROVER-derived and whole brain metabolic volumetric products (MVP) were significantly lower in AD and accurately distinguished AD patients from controls (Area Under the Curve (AUC) of Receiver Operator Characteristic (ROC) curves 0.89 and 0.86, respectively). This diagnostic accuracy was similar to voxel-based analyses. Analysis by ROVER of 18F-FDG-PET images provides a unique index of metabolically-active brain volume, and can accurately distinguish between AD patients and controls as a proof of concept. *In conclusion*, our findings suggest that ROVER may serve as a useful quantitative adjunct to visual or regional assessment and aid analysis of whole-brain metabolism in AD and other neurologic and psychiatric diseases.

## Introduction

Fluorine-18-fluorodeoxyglucose positron emission tomography (18F-FDG PET) imaging is a widely used modality for functional neuroimaging, and has shown particular utility in the diagnosis of neurodegenerative disease, including Alzheimer's disease (AD) [1, 2]. However, the quantitative analysis of 18F-FDG PET brain images in clinical practice is highly variable, the diagnosis relies primarily on visual inspection in most cases. Numerous advanced and powerful voxel-based image analysis techniques exist for brain 18F-FDG PET data which have demonstrated excellent diagnostic accuracy in a variety of neurologic conditions, in particular AD [3-6]. However, these methods often require coregistration of 18F-FDG PET data to structural magnetic resonance imaging (MRI) images, and require considerable specialized technical expertise, software, and time for off-line imaging processing, and have thus generally remained limited to research use. Region of interest (ROI) analysis is also widely used, but often requires a concurrent MRI for anatomical guidance [7-9], can be time intensive, and provides information only about the small regions of brain selected. A notable exception is the PALZ tool, which is an automated program which applies voxel-based statistical analysis to 18F-FDG images and has proven highly accurate in distinguishing AD images from control, suggesting that application of automated quantitative techniques to 18F-FDG images has clinical feasibility [5]. In 1993, Alavi et al. demonstrated a method for measuring whole brain total 18F-FDG uptake, by multiplying the MRI-acquired gray matter volume by the atrophy-corrected average metabolic rate of the brain [10]. This measure of global brain glucose uptake, termed the atrophy weighted total brain metabolism, showed a significant difference between AD patients and controls. However, the methods for determining whole brain 18F-FDG uptake remained cumbersome, and have thus not become widely employed in clinical practice.

Recently, our group has demonstrated the feasibility of using Region of interest visualization, evaluation, and image registration (ROVER, ABX, Radeburg, Germany) software to define the volume and global metabolic product of lung masses [11, 12]. The ROVER uses

a novel adaptive thresholding and background subtraction algorithm to identify lesion volume within a general user-defined search area (mask) [13]. Then ROVER applies partial volume correction, and provides volume, mean and max standardized uptake value (SUV), and metabolic volumetric product (mean SUVXvolume) data in an automated, non-biased manner, without MRI coregistration, image convolution, or ROI delineation. Importantly, ROVER analysis requires minimal expertise, can be applied to any image in minutes, and is already in clinical use in Europe. However, to our knowledge, ROVER analysis has never been applied to images of the brain in a systematic way. Thus, we hypothesized that ROVER analysis might be applicable to ^{18}F-FDG images of the brain, and might provide novel information about global brain metabolism. Further, this data might provide a clinically-facile means of quantitative measurement of whole-brain metabolic deficits in AD.

## Materials and methods

### Subjects

Patients were recruited and included in another imaging study described elsewhere [14], and PET images were subsequently analyzed separately for this study. Subjects with AD and controls were originally recruited from the Penn Memory Disorders Clinic/Alzheimer's Disease Center. Control and AD patients were matched for age and years of education. All patients underwent full neurocognitive testing in accordance with the Uniform Data Set of the National Alzheimer's Disease Coordinating Center [15]. Assessment included clinical dementia rating (CDR) Scale scoring. All controls had a CDR of 0 and a mini mental status score (MMSE)>27. All clinically diagnosed AD patients included in the study had a CDR of 0.5 or more, and a MMSE<25. Fluorine-18-FDG PET images from 18 control subjects and 14 AD patients were available and amenable to ROVER analysis. The mean age was 69.9±7.5 years for controls and 73.0±6.0 years for AD (n.s). Mean mini-mental status score at scan time was 29.3±1 of controls, 19.6±5.6 for AD (P<0.001). The mean CDR for AD patients was 1.04±0.72. Exclusion criteria included age <50 or >80, history of stroke or other known intracranial abnormality, clinically relevant abnormalities on routine bloodwork including glucose >200, contraindication to MRI or PET, and history of Axis I psychiatric disease or substance abuse.

### ^{18}F-FDG PET imaging

Positron emission tomography imaging was carried out based on the AD Neuroimaging Initiative (ADNI) PET imaging protocol [9]. Imaging was initiated approximately 40min after the intravenous administration of 185MBq of ^{18}F-FDG, and was conducted in a darkened, quiet room. Images were obtained on an Allegro scanner (Philips), as 4-5min scans. Images were reconstructed in the transaxial plane using an iterative reconstruction and [137]cesium transmission scan for attenuation correction.

Magnetic resonance imaging, segmentation, and volumetry: 3T high resolution T1-weighted and proton density images were acquired on the same day as ^{18}F-FDG-PET imaging. Segmentation was performed using a fuzzy connectedness method as previously described [16]. Briefly, MR images were corrected for inhomogeneity using in-house 3Dviewnix software (University of Pennsylvania, USA). The corrected imag-

es were then standardized over the entire dataset. Using the T2 image, cerebrospinal fluid (CSF) was segmented using the fuzzy connectedness operation in 3dviewnix. The same was done for gray matter and white matter, using the proton density image. After segmentation, affine registration was performed on the PET and MR images. The transformation was then applied to each of the previously obtained masks (CSF, Gray Matter and White Matter) to get the masks for the registered images. These registered images were then multiplied with the original PET image to get the masks (CSF, Gray Matter and White Matter) for the PET images.

### The use of ROVER for image analysis

For all analyses we used ROVER version 2.0.1 (ABX GmbH, Radeberg, Germany). A large spherical user-defined mask was drawn for each subject, which encompassed the entire brain and cerebellum in three dimensions. For cerebellar and cortex-only measurements, smaller masks which encompassed the cerebellum only or the deep grey nuclei (thalami, basal ganglia) were drawn (Fig. 1).
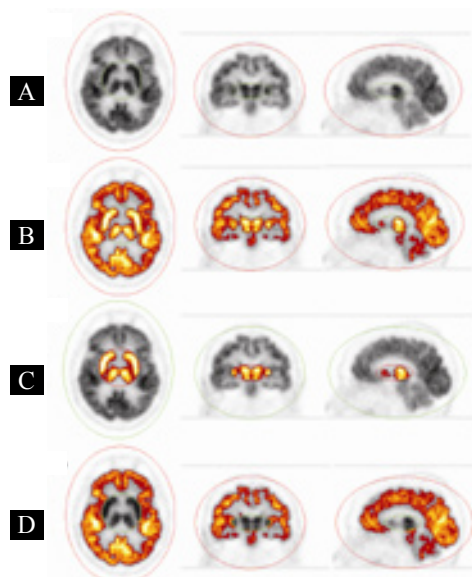


**Figure 1.** Images of ROVER whole brain and subregional volumes. A: Initial ^{18}F-FDG-PET images from a control subject showing user-drawn mask surrounding the whole brain and basal ganglia. B, C, D: Tissue identified by ROVER as metabolically active based on the whole brain (B), basal ganglia (C), and whole brain minus basal ganglia (cortex-only, D) masks. The original ^{18}F-FDG-PET image is shown in grayscale, while tissue identified by ROVER is in color.

Automatic ROI detection was employed using a initial threshold of 40% of the mask's maximum. This threshold provides the starting condition for an iterative process by determining tentative 3D ROI, which are further evaluated. For each tentative ROI a corresponding 3D background region was generated automatically in the close vicinity of the ROI. Starting from this initial estimate, a fully automatic procedure iteratively computes a background corrected threshold and the tentative ROI and corresponding background regions are modified accordingly. The iteration stops when all ROI volumes have converged. After convergence one or more 3D ROI result, for which all relevant parameters (volume, SUVmax, SUVmean etc.) are provided. All image analysis was performed with an initial threshold of 40% of the mask's maximum unless otherwise noted.

## Fluoro-18-FDG-PET voxel based, ROI analysis

^{18}F-FDG-PET images were coregistered with T1 MRI images using SPM5 (The Wellcome Department of Imaging Neuroscience, London, UK), then spatially normalized to Montreal Neurological Institute space with 2mm isotropic pixel size and smoothed with an isotropic kernel of 8mm. Region of interest analysis was performed based on the composite ROI developed for AD diagnosis for ADNI, which includes right and left angular gyri, bilateral posterior cingulate gyrus, and left middle/inferior temporal gyrus [9, 17]. Average voxel intensity in these ROI was normalized to whole-brain mean voxel intensity for that subject and reported in arbitrary units. All subjects were fasted for at least 6h prior to imaging, and blood glucose measurements were obtained at the time of imaging, all of which were between 70 and 110mg/dL.

## Results

### Volumetric analysis derived by ROVER in controls and AD

We first set out to determine if ROVER software could provide meaningful, accurate, and reproducible measurements from brain ^{18}F-FDG-PET images. As shown in Figure 1, ROVER analysis identified metabolically-active brain tissue in a pattern which, by visual inspection, correlated very closely with the initial ^{18}F-FDG-PET image. This required the user to generate only a simple spherical mask which grossly encompassed the whole brain, which could be drawn in a few seconds. The software also accurate identified subcortical grey matter nuclei or cerebellar hemispheres from smaller masks encompassing those structures (Fig. 1A-D). In AD patients, ROVER analysis with automatic ROI detection identified regions of normal or mildly diminished ^{18}F-FDG uptake, but severely hypometabolic regions in AD patients were excluded (Fig. 2). When the ROI detection method was changed from our default 40% automatic thresholding to a fixed threshold of 30% (of maximum voxel intensity within the mask), ROVER
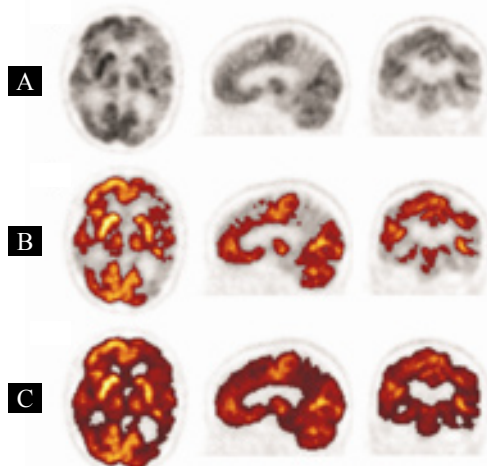
identified nearly all of the voxels which were apparent on the original ^{18}F-FDG PET image (see Fig. 2c). Thus, ROVER volumetric analysis using automatic ROI detection identified a "metabolic volume", i.e. the volume of metabolically active brain, rather than a true structural volume.

We next examined inter-rater reliability of whole brain volumetric measurements using ROVER. Comparison of values obtained independently by two different users demonstrated excellent reproducibility, as the concordance correlation coefficient was 0.959 (95% CI 0.918-0.979, pearson p (precision) 0.964, bias correction factor $C_b$ 0.995). Bland-Altman analysis, shown in Figure 3A, showed excellent clustering of values around the difference=0 line, and had a coefficient of repeatability of 73.74mm$^3$ (9% of the mean volume value). Thus, ROVER whole brain volumes were highly reproducible by two different users.

In order to validate the accuracy of brain volume measurement by ROVER, we next compared ROVER-derived brain volumes to MRI volumetric measurements. Magnetic resonance images from a subset of control (n=8) and AD patients (n=5) were subjected to segmentation using a fuzzy connectedness algorithm to define grey matter volume [16, 18]. This method allows highly accurate segmentation of grey matter, white matter, and CSF space and volume measurement without image convolution. Magnetic resonance imaging grey matter volumes were then compared to ROVER-derived cortex-only volumes, as ^{18}F-FDG uptake occurs primarily in the grey matter (Fig. 3B). Among control subjects, mean ROVER-derived cortex volume derived using automatic ROI detection differed by only 4.8% from MRI grey matter volumes (748±99cm$^3$ (MRI) vs. 720±106cm$^3$ (ROVER)). Moreover, control ROVER and MRI volumes correlated with an r$^2$ value of 0.93 and a slope of 0.87 (linear equation y(MRI)=0.87x(ROVER)-25.9). Interestingly, the mean ROVER-derived cortex volume (using automatic ROI detec-



**Figure 2.** Image of ROVER whole brain volume in an AD patient. A: Initial ^{18}F-FDG-PET image in grayscale. B: Tissue identified by ROVER as metabolically active using automatic ROI detection mode. Note the absence of ROVER signal in the bilateral parietal lobes on the AD patient due to low ^{18}F-FDG-PET intensity in this area. The original ^{18}F-FDG-PET image is shown in grayscale, while tissue identified by ROVER is in color. C: Tissue identified by ROVER using a fixed threshold mode with a preset threshold of 28% maximal pixel intensity.
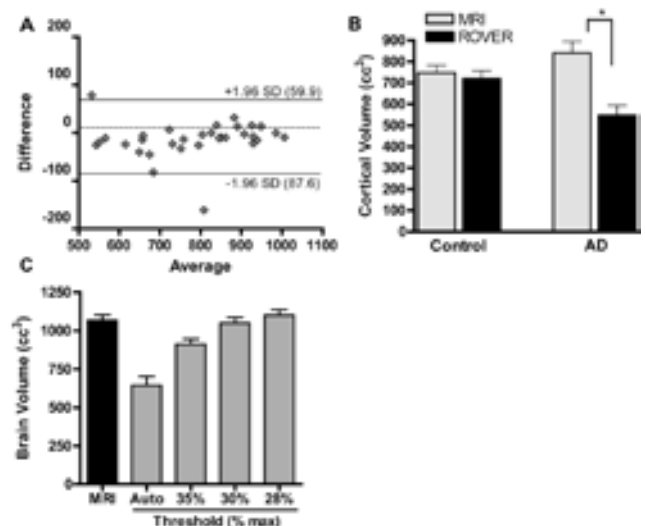


**Figure 3.** Inter-rater reliability and volumetric accuracy of ROVER. A: Bland-Altman difference vs. average plot of ROVER whole-brain measurement performed by two independent users. Solid lines show ±1.96 SD, while dotted line shows the difference/average ratio of 0. B: Cortical volumes derived from MRI (light gray) and ROVER-PET (black) in controls (left 2 bars) and AD patients (right 2 bars). C: Volume measurements from the patients from B. as obtained by MRI (black bars), ROVER in automatic ROI detection mode (auto), or ROVER in fixed-threshold mode with preset thresholds of 35, 30, or 28%. *P<0.05 by paired t-test.

tion mode) in AD patients was 35% less than mean MRI grey matter volume (840±124cm³ (MRI) vs. 547±106cm³ (ROVER), P<0.01 by paired t-test), as metabolically inactive brain tissue is excluded from the ROVER-derived "metabolically active" volume. These results demonstrate that ROVER-derived brain volume measurement closely correlates with MRI volumetry in normal brain, but as brain metabolism fails in AD, a substantial difference appears between MRI structural volume and ROVER-derived metabolic volume. Whole brain ROVER volumes were also determined using a fixed-threshold method. As shown in Figure 3c, analysis of AD brain volumes using a fixed threshold of 28% maximum (automatic ROI detection and iterative thresholding disabled) very closely approximated MRI-derived brain parenchyma volumes (3% difference, 1068±77cm³ (MRI) vs. 1100±82cm³ (ROVER), n.s.), showing that ROVER can also provide volume measurements that are very close to true structural volumes if automatic ROI detection is not employed.

### Metabolic volume measurement with ROVER in AD

Considering this pronounced difference in metabolically active brain volume on ROVER analysis between controls and AD patients, we next examined ROVER volumetric measurements in our full cohort of AD patients and controls. Volumetric ROVER analysis with automatic ROI detection was applied to whole brain, as well as to several brain subregions, including deep nuclei (basal ganglia, thalamus, and brainstem), cerebellum, and cerebral cortex (whole brain minus cerebellum and deep nuclei/brainstem). As expected, the whole brain ROVER-derived "metabolic volume" measure was significantly lower in AD patients than in controls (22.3% lower, P<0.01; see Fig. 4). Cerebral cortex metabolic volume was also significantly decreased in AD patients, and to a similar magnitude as whole brain (21.4%, P<0.01). However, cerebellar volumes were similar between groups, as the cerebellum is generally unaffected in AD. In order to assess the accuracy of diagnosis of ROVER-derived volumetric data, Receiver Operator Characteristic (ROC) curves were generated for both whole brain and cortex-only volumes. As showing in Figure 3, the Area Under the Curve (AUC) of the ROC curve was 0.89 for whole brain (89% accuracy, standard error 6%, P<0.001), while the AUC for cortex-only volume was 0.86 (86% accuracy, standard

error 7%, P<0.001). These findings suggest that ROVER volumetric measurement can detect global hypometabolism in AD, and that ROVER-derived whole brain and cortical volumes might serve as useful quantitative discriminators for the diagnosis of AD.

### Global SUV measurement in AD

Standardized uptake values (SUV) take into account patient weight and total radiation dose to provide a semi-quantitative indicator of cerebral metabolic rate, without the need for arterial blood sampling. ROVER automatically calculates the average SUV of a given volumes of interest (VOI), in this case the brain. We next examined ROVER-derived mean whole-brain SUV in AD and controls using automatic ROI detection. In this case, "whole brain" indicates all of the tissue which was identified by ROVER as metabolically active, which is a smaller volume of tissue in AD patients than controls. There were no significant differences between AD and controls in mean whole brain (8.6±2.2 control, 8.3±2.8 AD), cortical (8.6±2.2 control, 8.3±2.7 AD), or cerebellum (7.5±1.8 control, 7.6±2.1 AD) SUV. Thus, mean brain SUV did not discriminate between AD patients and controls. Because automatic ROI detection was employed, ROVER calculates mean SUV of brain tissue which has already been identified as metabolically active. Because the automatic thresholding feature of ROVER pre-selects only metabolically active tissue for inclusion in the mean SUV measurement, ROVER provides a mean SUV only of intact, metabolically active brain tissue, which of course does not discriminate AD from control.

### Global metabolic volumetric product measurements using ROVER in AD

A final measure of brain metabolism provided by ROVER is the whole brain metabolic volumetric product (MVP). This is calculated by multiplying the aforementioned volume measurement (metabolic volume) x the mean brain SUV, providing an index of whole brain ¹⁸F-FDG uptake, to which partial volume correction can be applied. Metabolic VP is useful in that it should be more sensitive to changes in subjects who have decreases in both metabolic volume and mean SUV. Metabolic VP was again calculated using automatic ROI detection for whole brain, cerebral cortex, and cerebellum
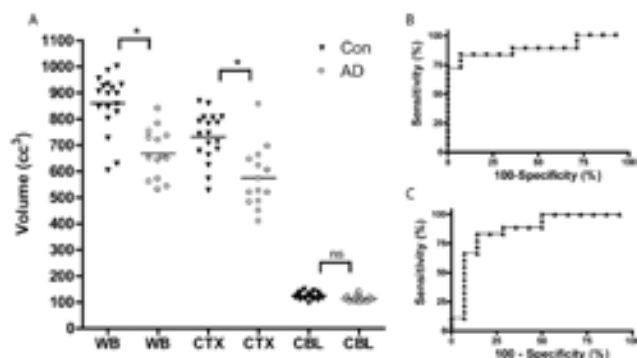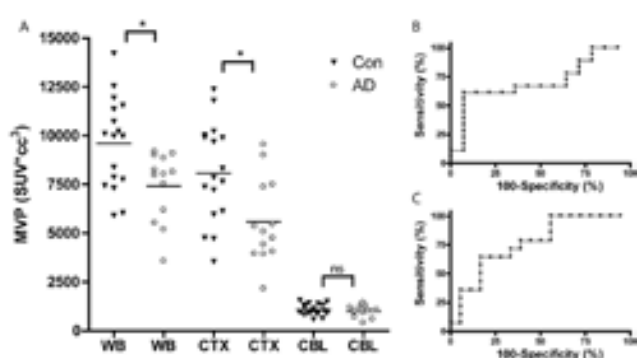


**Figure 4.** ROVER-derived volume measurements (metabolically-active brain volume) differentiate AD from control. A: Brain volumetric measurements from controls (black triangles) and AD patients (open circles). WB=whole brain, CTX=cortex only (WB-basal ganglia, cerebellum), CBL=cerebellum. B: ROC curve for ROVER whole brain volume measurements (AUC 0.89). C: ROC curve for ROVER cortex-only volume measurements (AUC 0.86). *P<0.01 by one-way ANOVA.



**Figure 5.** ROVER-derived metabolic volumetric product (MVP) measurements differentiate AD from control. A: Brain MVP measurements from controls (black triangles) and AD patients (open circles). WB=whole brain, CTX=cortex only (WB-basal ganglia, cerebellum), CBL=cerebellum. B: ROC curve for ROVER whole brain MVP measurements (AUC 0.71). C: ROC curve for ROVER cortex-only MVP measurements (AUC 0.77). P<0.01 by one-way ANOVA.

(Fig. 5). As expected, whole brain MVP was 21.1% lower in AD patients than controls (P<0.01), and cerebral cortex MVP showed an even larger difference between groups (31.6% decrease in AD, P<0.01). Cerebellar MVP was not significantly different between groups.

## Comparison of ROVER analysis to SPM-based ROI analysis

We next compared the accuracy of ROVER analysis to the widely-employed region of interest-based method of Landau et al (2010, 2009), which has previously been validated [17, 19]. The Landau method uses voxel-based analysis to quantify metabolism in 5 predefined regions (bilateral temporal and parietal lobes and anterior cingulate) which have been demonstrated by literature meta-analysis to be the voxels which are most commonly hypometabolic in AD on ^{18}F-FDG-PET. Fluorine-18-FDG-PET images were normalized to the Montreal Neurologic Institute brain atlas, then subjected to voxel-based analysis with SPM5 using the Landau et al. ROI. As shown in Figure 6, this method showed a mean 26.7% difference between AD and controls (P<0.01 by t-test). ROC curve analysis produced an AUC of 0.85 (SE 0.08, 95% confidence interval 0.69-1.01, P=0.0012). These numbers were very similar to those derived from both ROVER metabolic volume measurement, as well as ROVER MVP analysis, suggesting that in this small sample, ROVER performs with similar accuracy as a previously-validated ROI-based method, without need for image normalization or voxel-based analysis.

## Correlation of ROVER-derived measurements with clinical dementia rating (CDR)

We next examined the correlation between clinical dementia rating (CDR) and ROVER measurements. We grouped our patients into 3 sets: CDR 0 (cognitively normal), CDR 0.5 (very mild dementia), and CDR 1 or greater (CDR 1+, mild dementia or worse), and compared ROVER whole brain metabolic volume. As shown in Figure 7, the mean ROVER whole brain volume decreased as CDR increased. There was a statistically significant difference between the CDR 0 and CDR 1+ group (P<0.05 by one-way ANOVA). The CDR 0.5 group did not meet statistical significance, as there were only 6 patients in this group, though there was clearly a trend toward decreased volume as compared to CDR 0, but not as severe as CDR 1+.
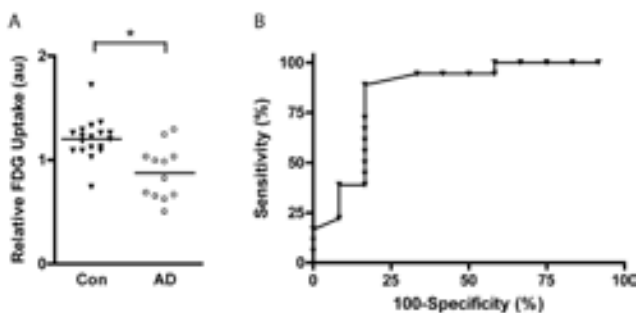
## Discussion

In this communication we examined a novel method for the measurement of global cerebral metabolic activity from ^{18}F-FDG PET images using ROVER software. This method is facile enough for use in the clinical setting, and provides a novel measure of metabolic volume, as well as metabolic volumetric product, which provide unique quantitative information about global brain metabolism. As proof of concept, we have applied this method in a pilot cohort of patients with AD and controls, and demonstrated that both MV and MVP distinguish these groups with excellent accuracy. ROVER analysis was similar in accuracy to a validated ROI-based method, and MV declines as clinical dementia rating increases. Thus, we conclude that ROVER analysis of ^{18}F-FDG-PET brain images has considerable promise for the study of global cerebral metabolism in AD and other neurologic disorders.

Classically, ^{18}F-FDG-PET has been used to detect regional hypometabolism in AD, particularly in affected regions such as the posterior cingulate, parietal, and occipital lobes [20]. This has generally been achieved through measurement of multiple ROI (either manually placed or automated), or voxel-based analysis [8, 21, 22]. However, a previous report demonstrated the feasibility of calculating atrophy-corrected whole brain ^{18}F-FDG uptake, and showed that this measure could readily distinguish AD patients from controls [10]. This early method was rudimentary in it estimates of the average metabolic activity of the brain, and required MRI for volume determination. ROVER software allows automated determination of atrophy corrected whole brain ^{18}F-FDG uptake without concurrent MRI data, and differentiates AD from controls in our cohort with similar accuracy as a validated ROI-based method. Thus, ROVER makes measurement of global cerebral metabolism feasible on a large scale. ROVER-based whole brain ^{18}F-FDG uptake measurement is attractive for use in neuroimaging for several reasons. Global measurements might detect subtle, diffuse changes in metabolism, or changes that occur in tissue not contained within the boundaries of a pre-selected ROI. Furthermore, ROVER does not require deformation of images to fit a standard atlas, which can induce error in atrophied brain, or significant offline processing, as is needed in SPM analysis. Thus, ROVER-based global analysis might complement existing regional methods, a possibility which should be investigated in future studies. The three objective parameters could be valuable adjuncts to the visual assessment method and
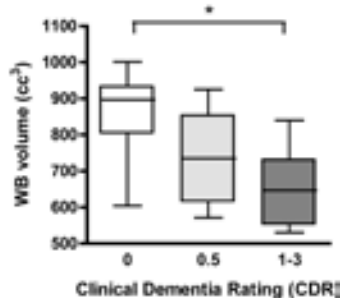
**Figure 6.** Voxel-based Region of Interest (ROI)-based analysis of ^{18}F-FDG-PET data. A: Relative ^{18}F-FDG uptake for control and AD patients derived from voxel-based composite ROI method. Voxel intensity in 5 ROI were normalized to whole-brain voxel intensity and reported in arbitrary units. B: ROC curve for Landau ROI data. AUC is 0.85. *P<0.01 by 2-tailed t-test.

**Figure 7.** Relationship of ROVER whole brain metabolic volume to Clinical Dementia Rating. Whole brain (WB) volume measurements were grouped by CDR=1 (no dementia), CDR=0.5 (mild impairment), and CDR>0.5 (moderate to severe dementia). *P<0.05 by 2-tailed t-test.

could be hopefully adopted in the same patient to monitor disease course and the efficacy of novel therapies.

The ability of ROVER analysis to discriminate AD patients from controls lies primarily in the fact that regions of minimal metabolic activity are excluded from the ROVER volume measurements. This is demonstrated by our finding that in controls, ROVER metabolic volume and MRI-derived cortical volume are nearly identical, while in AD patients, ROVER metabolic volume is on average 35% lower than structural measurements. However, when a fixed-threshold ROI detection method is employed, ROVER can derive whole brain volumes which are very similar to those obtained with MRI imaging, suggesting that ROVER might be useful for estimating both structural and metabolic volume from ^{18}F-FDG-PET images. The ratio of structural (MRI derived) to metabolic (PET-ROVER derived) volume might thus provide another unique biomarker of AD, and is an avenue for future study.

The clinical utility of ^{18}F-FDG-PET for the diagnosis of AD in clinical practice is mitigated by the variability of qualitative reads. Even expert nuclear medicine physicians can vary considerably in their sensitivity and specificity for the diagnosis of AD by visual inspection of ^{18}F-FDG-PET images [14]. Thus, there is a pressing need for quantitative image analysis methods which are accurate, yet clinically applicable. Considering the reproducibility or ROVER measurements and the minimal amount of user input required to obtain these measures (images can be fully analyzed in less than 2min with minimal training), ROVER analysis could have potential clinical applicability in the future.

ROVER analysis is particularly powerful because it can be applied to any image in DICOM format. Thus, ROVER could potentially be employed to quantify whole brain amyloid burden from images employing amyloid-binding PET ligands such as Pittsburgh Compound B or Florbetapir [23, 24]. ROVER analysis could also be used to derive accurate, partial volume corrected striatal volumes from ^{18}F-DOPA images, which could potentially be useful in the diagnosis of Parkinson's disease. Furthermore, ROVER analysis of ^{18}F-FDG PET images also have possible uses in other diseases of the brain, such as depression, schitzophrenia, or metabolic disorders, in which diffuse changes in brain metabolism might be present [25-27]. Ongoing efforts in our lab are aimed at exploring some of these possibilities.

There are several potential disadvantages to ROVER analysis. First, signal from highly focal metabolic changes could be diluted in global analysis. Thus, ROVER may not be ideal for disease processes which are highly focal, unless a particular anatomic structure was consistently involved which could be contained within a ROVER mask. ROVER analysis must also be examined in a more heterogeneous population with a mix of neurologic diseases, as would be seen in clinical practice. It is possible that multiple neurologic diseases could have decreases in global metabolism on ROVER analysis that might overlap, clouding diagnostic differentiation. The diagnostic accuracy of ROVER in combination with classic visual pattern recognition and region of interest-based methods in a mixed population of neurologic disorder should be examined in future studies to address this issue. Nonetheless, in the same subject, this value could be quite robust to monitor disease course and efficacy of novel approaches. This study was intended as a pilot investigation of ROVER analysis in AD patients, and was thus not designed or powered to provide evidence of diagnostic superiority or

equivalence to other image analysis methods. The comparison to the Landau et al voxel-based ROI method provides only a general estimate that ROVER performs comparably to this previously-validated method in our small cohort. The accuracy of ROVER analysis and the comparison to other image analysis methods will need to be examined in larger cohorts.

*In conclusion*, we have examined the feasibility of a novel method for quantification of whole brain glucose metabolism using ROVER software. This method accurately differentiates AD patients from control subjects, demonstrating the potential utility of global metabolic measures in the diagnosis and monitoring of AD or other neurologic diseases. Our findings also illustrate the promise of ROVER analysis of PET images as a complimentary approach in future investigations of neurodegeneration or even in clinical practice.

*The authors declare that they have no conflicts of interest.*

## Bibliography

1. Mosconi L. Brain glucose metabolism in the early and specific diagnosis of Alzheimer's disease. FDG-PET studies in MCI and AD. *Eur J Nucl Med Mol Imaging* 2005; 32: 486-510.
2. Silverman DH, Small GW, Chang CY et al. Positron emission tomography in evaluation of dementia: Regional brain metabolism and long-term outcome. *Jama*, 2001; 286: 2120-7.
3. Signorini M, Paulesu E, Friston K et al. Rapid assessment of regional cerebral metabolic abnormalities in single subjects with quantitative and nonquantitative [^{18}F]FDG PET: A clinical validation of statistical parametric mapping. *Neuroimage* 1999; 9: 63-80.
4. Salmon E, Collette F, Degueldre C et al. Voxel-based analysis of confounding effects of age and dementia severity on cerebral metabolism in Alzheimer's disease. *Hum Brain Mapp* 2000; 10: 39-48.
5. Herholz K, Salmon E, Perani D et al. Discrimination between Alzheimer dementia and controls by automated analysis of multicenter FDG PET. *Neuroimage* 2002; 17: 302-16.
6. Ishii K, Sasaki H, Kono AK et al. Comparison of gray matter and metabolic reduction in mild Alzheimer's disease using FDG-PET and voxel-based morphometric MR studies. *Eur J Nucl Med Mol Imaging* 2005; 32: 959-63.
7. Smith GS, de Leon MJ, George AE et al. Topography of cross-sectional and longitudinal glucose metabolic deficits in Alzheimer's disease. Pathophysiologic implications. *Arch Neurol* 1992; 49: 1142-50.
8. Mosconi L, Tsui WH, De Santi S et al. Reduced hippocampal metabolism in MCI and AD: automated FDG-PET image analysis. *Neurology* 2005; 64: 1860-7.
9. Jagust WJ, Bandy D, Chen K et al. The Alzheimer's Disease Neuroimaging Initiative positron emission tomography core. *Alzheimers Dement* 2010; 6: 221-9.
10. Alavi A, Newberg AB, Souder E, Berlin JA. Quantitative analysis of PET and MRI data in normal aging and Alzheimer's disease: atrophy weighted total brain metabolism and absolute whole

brain metabolism as reliable discriminators. *J Nucl Med* 1993; 34: 1681-7.

11. Torigian DA, Chong E, Schuster S et al. Feasibility and utility of ROVER software for 3D quantitative image analysis of FDG-PET in patients with diffuse large B-cell lymphoma (DLBCL). *J Nucl Med* 2009; 50: 135.

12. Torigian DA, Lopez RF, Alapati S et al. Feasibility and performance of novel software to quantify metabolically active volumes and 3D partial volume corrected SUV and metabolic volumetric products of spinal bone marrow metastases on 18F-FDG-PET/CT. *Hell J Nucl Med* 2011; 14: 8-14.

13. Hofheinz F, Potzsch C, Oehme L et al. Automatic volume delineation in oncological PET. Evaluation of a dedicated software tool and comparison with manual delineation in clinical data sets. *Nuklearmedizin* 2011; 51(1): 9-16.

14. Musiek ES, Chen Y, Korczykowski M et al. Direct comparison of FDG-PET and ASL-MRI in Alzheimer's Disease. *Alzheimer's and Demenia* 2012; 8(1) 51-9.

15. Morris JC, Weintraub S, Chui HC et al. The Uniform Data Set (UDS): clinical and cognitive variables and descriptive data from Alzheimer Disease Centers. *Alzheimer Dis Assoc Disord* 2006; 20: 210-6.

16. Udupa JK, Nyul LG, Ge Y, Grossman RI. Multiprotocol MR image segmentation in multiple sclerosis: experience with over 1,000 studies. *Acad Radiol* 2001; 8: 1116-26.

17. Landau SM, Harvey D, Madison CM et al. Comparing predictors of conversion and decline in mild cognitive impairment. *Neurology* 2010; 75: 230-8.

18. Moonis G, Liu J, Udupa JK, Hackney DB. Estimation of tumor volume with fuzzy-connectedness segmentation of MR images. *Am J Neuroradiol* 2002; 23: 356-63.

19. Landau SM, Harvey D, Madison CM et al. Associations between cognitive, functional, and FDG-PET measures of decline in AD and MCI. *Neurobiol Aging* 2011; 32(7): 1207-18.

20. Mosconi L, Tsui WH, Rusinek H et al. Quantitation, regional vulnerability, and kinetic modeling of brain glucose metabolism in mild Alzheimer's disease. *Eur J Nucl Med Mol Imaging* 2007; 34: 1467-79.

21. Chetelat G, Desgranges B, Landeau B et al. Direct voxel-based comparison between grey matter hypometabolism and atrophy in Alzheimer's disease. *Brain* 2008; 131: 60-71.

22. Li Y, Rinne JO, Mosconi L et al. Regional analysis of FDG and PIB-PET images in normal aging, mild cognitive impairment, and Alzheimer's disease. *Eur J Nucl Med Mol Imaging* 2008; 35: 2169-81.

23. Klunk WE, Engler H, Nordberg A et al. Imaging brain amyloid in Alzheimer's disease with Pittsburgh Compound-B. *Ann Neurol* 2004; 55: 306-19.

24. Wong DF, Rosenberg PB, Zhou Y et al. In vivo imaging of amyloid deposition in Alzheimer disease using the radioligand 18F-AV-45 (florbetapir [corrected] F 18). *J Nucl Med* 2010; 51: 913-20.

25. Kumar A, Newberg A, Alavi A et al. Regional cerebral glucose metabolism in late-life depression and Alzheimer disease: a preliminary positron emission tomography study. *Proc Natl Acad Sci U SA* 1993; 90: 7019-23.

26. Gur RE, Resnick SM, Alavi A et al. Regional brain function in schizophrenia. I. A positron emission tomography study. *Arch Gen Psychiatry* 1987; 44: 119-25.

27. Seo SW, Lee BI, Lee JD et al. Thyrotoxic autoimmune encephalopathy: a repeat positron emission tomography study. *J Neurol Neurosurg Psychiatry* 2003; 74: 504-6.